Journal of Medicines Development Sciences, 2026, Volume 11, Issue 3
https://bbwpublisher.com/journal/JMDS
ISSN Online:2382-6371
ISSN Print:2382-6363

The Effect of Muscone on Lipopolysaccharide-Induced Damage to Human Umbilical Vein Endothelial Cells

Miao Li*

College of Pharmacy, Qilu Medical University, Zibo 255000, Shandong, China

***Corresponding author:** Miao Li, 119934977@qq.com

Copyright: © 2026 Author(s). This is an open-access article distributed under the terms of the Creative Commons Attribution License (CC BY 4.0), permitting distribution and reproduction in any medium, provided the original work is cited.

Abstract: *Objective:* To investigate the role and mechanism by which musk ketone modulates the NLRP3/Caspase-1/GSDMD signaling pathway to intervene in lipopolysaccharide (LPS)-induced pyroptosis in human umbilical vein endothelial cells (HUVECs). *Methods:* The CCK-8 assay was used to screen for the safe and effective concentration of musk ketone. HUVECs were divided into a control group, a model group, and low-, medium-, and high-dose musk ketone groups. A pyroptosis model was established by stimulating cells with 10 μg/mL LPS for 16 h, and each dose group was treated with musk ketone for 24 h. The NO level, inflammatory cytokine expression, and protein levels in the pyroptosis pathway were assessed using an NO assay kit, ELISA, and Western blot, respectively. *Results:* Musk ketone at concentrations ranging from 1 to 75 μmol/L exhibited no significant cytotoxicity. NO measurements revealed that NO levels in the cell supernatant were significantly higher in the model group compared to the control group. Additionally, Western blot analysis showed that the expression levels of NLRP3, Caspase-1, and GSDMD proteins were elevated in the model group compared to the control group, collectively confirming that LPS successfully induced pyroptosis and inflammatory damage in endothelial cells. ELISA results showed that the expression levels of IL-18 and IL-1β in the model group were significantly higher than those in the control group ($P < 0.05$); compared with the model group, the high-, medium-, and low-concentration muskon groups all showed a significant reduction in IL-18 expression in cells ($P < 0.05$); compared with the model group, the high- and low-concentration muskon groups both showed a significant reduction in IL-1β expression in cells ($P < 0.05$). Western blot results showed that, compared with the control group, the model group exhibited increased expression of NLRP3, Caspase-1, and GSDMD proteins in cells ($P < 0.01$). Compared with the model group, the high-, medium-, and low-dose muscone groups all exhibited significantly reduced expression of NLRP3, Caspase-1, and GSDMD proteins in cells ($P < 0.05$). *Conclusion:* Musk ketone can effectively inhibit LPS-induced pyroptosis in human umbilical vein endothelial cells and suppress cellular inflammatory damage by inhibiting the NLRP3/Caspase-1/GSDMD signaling pathway and reducing the release of inflammatory factors.

Keywords: Muscone; Pyroptosis; NLRP3/GSDMD/Caspase-1; Inflammatory factors

Online publication: September 16, 2026

1. Introduction

Diabetes mellitus (DM) is a chronic metabolic disorder, and diabetic foot ulcers are a common complication of this condition [1]. Diabetic wounds are typically characterized by a high incidence rate, slow healing, and a prolonged course of the disease that makes closure difficult. This not only significantly impairs the quality of life for people with diabetes but also causes long-term damage to various bodily functions. After the hemostasis phase of a diabetic wound is complete, the inflammatory phase often subsides slowly, and oxidative stress levels rise, thereby slowing wound healing [2]. An uncontrolled, excessive inflammatory response is the core pathological factor hindering the healing of diabetic ulcers, and pyroptosis—which releases large amounts of pro-inflammatory factors—is the primary cause of the wound's prolonged, hyper-inflammatory state [3].

Pyroptosis is a novel programmed cell death pathway regulated by the pore-forming protein GSDMD (GSDMD). It is primarily controlled by caspase-1, which simultaneously releases sufficient amounts of pro-inflammatory factors—the precursors of IL-1β and IL-18—while the expression levels of genes encoding inflammasome-related proteins also increase. Once the signaling pathway is fully activated, the process enters the activation phase, the core components of which are inflammasome complex assembly and caspase activation [4,5]. Among the various relevant studies to date, the mechanism of action of the NLRP3 inflammasome has been analyzed most comprehensively and thoroughly. The NLRP3 protein recruits the inactive Caspase-1 precursor (pro-Caspase-1), thereby completing the assembly of the NLRP3 inflammasome;pro-Caspase-1 is converted into catalytically active mature Caspase-1 through autolytic modification; the activated Caspase-1 cleaves the GSDMD protein, splitting it into two peptide fragments: GSDMD-N and GSDMD-C.GSDMD-N selectively binds to lipids on the inner surface of the cell membrane, forming membrane channels with pore sizes of 10 to 15 nanometers on the cell surface. This disrupts the osmotic balance between the intracellular and extracellular environments, ultimately leading to cell swelling and rupture—a form of cell death known as pyroptosis. During this process, large amounts of mature IL-1β and IL-18 are released into the extracellular space, amplifying the inflammatory response in a cascading manner and triggering a chain reaction known as the inflammatory cascade. Within the non-canonical pyroptosis signaling pathway, bacterial lipopolysaccharide (LPS) can directly bind to Caspase-4, Caspase-5, and Caspase-11, thereby activating these proteases. Activated Caspase-4/5/11 exert bidirectional regulatory effects: on the one hand, they directly cleave GSDMD to produce GSDMD-N, which creates pores in the cell membrane, leading to cell membrane rupture and inducing pyroptosis; on the other hand, they enhance NLRP3 inflammasome activity, indirectly activating Caspase-1, which in turn catalyzes the synthesis and secretion of mature IL-1β and IL-18 [6], thereby exacerbating various inflammatory responses in the body.

Pyroptosis is a synergistic process involving innate immunity and inflammation that is activated to defend the body against invading pathogenic microorganisms. When occurring in moderation, pyroptosis can eliminate various pathogenic microorganisms after they invade the body; however, numerous studies have shown that this physiological process has both benefits and drawbacks. Excessive activation of pyroptosis can induce persistent inflammatory stimulation, leading to skin ulcers and wounds that are difficult to heal over the long term.IL-1β and IL-18 are highly representative inflammatory molecules; existing literature suggests that IL-1β can also amplify the physiological effects of other inflammatory mediators [7]. Research by Wang Tao's team found that in skin wounds of diabetic patients, the protein and gene expression levels of NLRP3, Caspase-1, and IL-1β are significantly upregulated at both the protein and gene transcription levels, which readily triggers excessive inflammation in macrophages under a hyperglycemic environment and in

diabetic wounds. This weakens insulin responsiveness, damages vascular endothelial tissue, and delays the wound healing process. Intervening in this inflammatory signaling pathway could serve as a novel research direction for the treatment of diabetic skin ulcers [8]. Research by Jiang Fangyang has confirmed that Polysaccharides from Yuzhu can downregulate the expression of proteins associated with the NLRP3 inflammasome, block pyroptosis and apoptosis, and reduce inflammatory damage to kidney tissue in a diabetic nephropathy mouse model, thereby achieving therapeutic effects in intervening against nephropathic lesions. Zhou Jun's experimental results show that rhodiolide can lower blood glucose levels in experimental mice with type 2 diabetes. By activating adenylate-activated protein kinase, it inhibits the abnormally activated NLRP3 signaling pathway in the liver; simultaneously, by blocking the NLRP3/GSDMD signaling pathway, it reduces pyroptosis in pancreatic β-cells of experimental mice [10]. Wang Xianfeng and her team demonstrated that the NLRP3 inflammasome is fully involved in the progression of diabetic foot lesions; inhibiting the abnormal activation of this complex helps improve clinical recovery outcomes for patients with diabetic foot [11].

Traditional medicine possesses unique advantages, such as multi-pathway and multi-site regulation, as well as minimal adverse reactions. It can block the pyroptosis activation process, alleviate systemic inflammatory damage, and repair organ pathological damage caused by complications, thereby slowing disease progression and playing a reliable role in the clinical prevention and treatment of diabetes and its various complications. The use of active components and extracts from natural medicinal materials to modulate cellular pyroptosis as an intervention for diabetes and related complications has been a hot topic of research in recent years [4].

Musk (Moschus) is derived from the air-dried secretions found in the glandular sacs of adult male forest musk deer, horse musk deer, and the original musk deer. The scientific name for the original musk deer is *Moschus moschiferus Linnaeu*s; for the forest musk deer, it is *Moschus berezovskii Flerov*; and for the horse musk deer, it is *Moschus sifanicus Przewalski* [12]. Existing experimental data indicate that musk can protect both the cardiovascular and central nervous systems, and also possesses diverse pharmacological effects, including antitumor activity, uterine stimulation, anti-inflammatory effects, and acceleration of uterine contractions. Regarding inflammation regulation, musk exhibits potent, broad-spectrum anti-inflammatory effects throughout all phases of the inflammatory response, with stable and reliable clinical efficacy [13]. Musk ketone is the core active component responsible for the anti-inflammatory effects of natural musk [14]. This substance is the core pharmacologically active component of musk; its full chemical name is 3-methylcyclopentadiene. It appears as a pale yellow or transparent oily liquid, has an odor highly similar to that of the raw herbal material, and exhibits clinical effects largely comparable to those of natural musk [15]. Research by Shi Yaqi's team suggests that musk ketone can block inflammatory activation triggered by the NLRP3 inflammasome within myocardial cells, alleviate myocardial lesions in mice with a lipopolysaccharide-induced sepsis model, and restore impaired cardiac physiological function [16]. Existing literature has demonstrated that the pyroptosis pathway regulated by the NLRP3/Caspase-1 signaling axis is a classic mechanism of pyroptosis[17]. Based on the conclusions from the above literature, this study hypothesizes that musk ketone can regulate the NLRP3/Caspase-1/GSDMD pyroptosis signaling pathway to accelerate the repair and healing of diabetic skin ulcers.

Lipopolysaccharides (LPS) constitute a key structural component of the outer membrane of Gram-negative bacilli, which are highly prevalent pathogenic microorganisms in infected wounds [18]. Various studies have confirmed that high sugar levels, high blood lipids, and lipopolysaccharide stimulation all

activate inflammatory responses in the body, inducing pyroptotic damage in target cells associated with diabetic pathologies; these are key factors contributing to cellular damage that leads to complications [19]. Experiments by Tian Xinru's team confirmed that treating cells with LPS at a concentration of 10 μg/mL for 16 hours is an appropriate condition for establishing a model of cellular inflammatory damage [20].

Endothelial cells (ECs) form a single-layered, multifunctional cell layer that closely adheres to the vascular wall. Located in the intima layer of the blood vessel, they act as a barrier separating circulating blood from surrounding tissues; endothelial cells regulate blood flow velocity and the degree of vasoconstriction, exert both anticoagulant and procoagulant effects, and participate in lipoprotein metabolism. Endothelial cells constitute the body's largest endocrine system, capable of synthesizing and secreting more than ten types of bioactive substances; they regulate systemic immune activity by releasing various cytokines. An intact vascular endothelial architecture is a fundamental prerequisite for maintaining the stable functioning of the endothelium's various physiological functions; endothelial cells themselves are highly susceptible to damage caused by various inflammatory factors. Therefore, these cells are frequently used to elucidate the underlying mechanisms by which inflammatory stimuli cause cellular damage. She Xu and colleagues used human umbilical vein endothelial cells as an experimental model and demonstrated that lipopolysaccharide (LPS) can induce inflammatory responses in the vascular endothelium and trigger tissue damage [21].

When Liu Pengfei's team investigated the combined use of muscone and bone marrow-derived mesenchymal stem cells to treat acute kidney injury in rats, they employed the CCK-8 assay to test multiple dose gradients of muscone, observe changes in stem cell proliferative activity, define the safe therapeutic range of the drug, and establish the following dose groups: low concentration 0.3 mg/L, medium concentration 1.0 mg/L, and high concentration 3.0 mg/L [22]. This study conducted preliminary pre-trials based on this dosage regimen, using the CCK-8 assay to screen for the effective concentration range of muscone suitable for human umbilical vein endothelial cells.

In this study, human umbilical vein endothelial cells were selected for in vitro experiments. Lipopolysaccharide (LPS) was used to induce inflammatory damage in the cells. After subculturing the cells, they were treated with different concentrations of musk ketone, and the levels of intracellular inflammatory factors IL-1β and IL-18 were measured using the ELISA method. Protein immunoblotting was used to measure the expression levels of pyroptosis-related proteins NLRP3, Caspase-1, and GSDMD, thereby elucidating the intrinsic molecular mechanism by which musk ketone regulates LPS-induced pyroptosis in endothelial cells via the NLRP3/Caspase-1/GSDMD signaling pathway.

2. Experimental design and protocol

2.1. Instruments, reagents, and consumables

Table 1. List of Major Instruments and Equipment

Major Instruments and Equipment	Manufacturer	Specifications and Model
Refrigerator	Haier Refrigerator Co., Ltd.	BCD477WGHHDDSP
Microscope	ECHO, USA	REB-01
0.0001-gram balance	Hunan Lichen Instrument Technology Co., Ltd.	Lichen FA224
Ice Maker	Changshu Xueke Electrical Appliances Co., Ltd.	LMS-30
Medical Clean Bench	Jinan Xinbeixi Biotechnology Co., Ltd.	BBS-SDC

Major Instruments and Equipment	Manufacturer	Specifications and Model
Cell Culture Incubator	Singapore Yisigao Life Sciences Group	CCL-170B-8
Centrifuge	CelloTec, Inc., USA	TDZ5
Vortex Mixer	CelloTec, Inc., USA	SCI-VS(MX-S)
Microcentrifuge	Eppendorf AG, Germany	S1010E
Electric 8-Channel Pipette	Eppendorf AG, Germany	Xplorer
Continuously Adjustable Single-Channel Pipette	Eppendorf AG, Germany	ResearchPlus
Digital Circular Shaker	CelloTec, Inc., USA	SLK-O3000-S
Chemiluminescence Instrument	Roche Diagnostics, Inc.	4800
Metal Bath	CelloTec, Inc., USA	SCI120-S
Electrophoresis System	Jiangsu Huanuota Biomedical Co., Ltd.	HT-300
Microplate Reader	Xinbeixi Biotechnology Co., Ltd.	HBS-1096C
Cell Disruptor	Ningbo Xinzhi Biotechnology Co., Ltd.	JY92-IIDN

Table 2. List of Test Reagents and Consumables

Reagents and Consumables	Manufacturer	Catalog Number
Human Umbilical Vein Endothelial Cells	Shanghai McLean Biotechnology Co., Ltd.	XY-M034
Universal Cell Cryopreservation Medium	Aopai Bio-Technology (Shanghai) Co., Ltd.	C00250
PBS Buffer	Aopai Bio-Technology (Shanghai) Co., Ltd.	ORCPB0521
IL-18 ELISA Kit	Jiangsu Jingmei Biotechnology Co., Ltd.	JM-023231
IL-1β ELISA Kit	Jiangsu Jingmei Biotechnology Co., Ltd.	JM-023267
β-Actin Internal Control	Hangzhou Hua'an Biotechnology Co., Ltd.	PJH78601
Anti-human GSDMD primary antibody	Wuhan Yunclone Technology Co., Ltd.	PAT529hu01
Anti-human NLRP3 primary antibody	Wuhan Yunclone Technology Co., Ltd.	PAK115hu01
Anti-human Caspase-1 Antibody	Wuhan Yunclone Technology Co., Ltd.	PAB592hu01
Anti-human IL-1β Antibody	Wuhan Yunclone Technology Co., Ltd.	PAA563hu01
Goat Anti-Rabbit Immunoglobulin G Secondary Antibody	Wuhan Yunclone Technology Co., Ltd.	HA1001
Protein Loading Buffer (1X)	Hefei Lanjieke Technology Co., Ltd.	BL1010A
Protein Loading Buffer (5X)	Beijing Lanbolide Trading Co., Ltd.	G2527
RIPA Lysis Buffer	Beijing Lanbolide Trading Co., Ltd.	R1091
PMSF	Beijing Lanbolide Trading Co., Ltd.	R109-B
BCA Protein Concentration Assay Kit	Shanghai Hongye Biotechnology Co., Ltd.	GK1000
SDS-PAGE AB Solution Rapid Gel Preparation Kit	Beijing Lanbolide Trading Co., Ltd.	P0105
Blotting Buffer	Beijing Lanbolide Trading Co., Ltd.	Z0202M
Electrophoresis Solution	Beijing Lanbolide Trading Co., Ltd.	T7777
TBST Buffer	Beijing Lanbolide Trading Co., Ltd.	T9040
ECL Developer	Hefei Lanjieke Technology Co., Ltd.	BL520A
Primary Antibody Dilution Solution	Beijing Lanbolide Trading Co., Ltd.	D0151
Secondary Antibody Dilution Buffer	Shanghai Biyuntian Biotechnology Co., Ltd.	P0023D
Skim Milk Powder	Beijing Lanbolide Trading Co., Ltd.	N7861
Musk ketone	Shanghai Haohong Biomedical Technology Co., Ltd.	1079699
Premium Fetal Bovine Serum	Jinclone (Beijing) Biotechnology Co., Ltd.	CF0030
Specialized Culture Medium for HUVEC Cells	Shanghai Xinyu Biotechnology Co., Ltd.	XY-HM205

2.2. Research methods

2.2.1. Screening of the usable concentration range of musk ketone using the CCK-8 assay

2.2.1.1. Preliminary cell assay

The CCK-8 assay was used to evaluate the effects of different concentrations of musk ketone on the viability of human umbilical vein endothelial cells. The specific steps are as follows:

Seed the prepared human umbilical vein endothelial cell suspension into a 96-well plate (100 μL per well), with three replicate wells per group; after the cells have adhered, treat them with 1 μmol, 5 μmol, 10 μmol, 25 μmol, 50 μmol, or 75 μmol of musk ketone for 24 hours according to the groupings described above; Prepare a mixture of CCK-8 reagent and serum-free DMEM medium. Discard the residual medium from the culture plates and add 100 μL of the mixture to each well, taking care to avoid creating bubbles. Return the plates to the cell culture incubator for further incubation for 1–4 hours; Place the 96-well plates into a microplate reader and measure the absorbance at a wavelength of 450 nm; Calculate the change in cell viability for each group after treatment using the formula.

Cell Viability (%) = [(As – Ab) / (Ac – Ab)] × 100%

As: Absorbance of the experimental well (containing human umbilical vein endothelial cells treated with muscone, along with culture medium and CCK-8 reagent)

Ac: Absorbance of the control well (containing normally cultured human umbilical vein endothelial cells, culture medium, and CCK-8 reagent)

Ab: Absorbance of the blank well (containing only culture medium and CCK-8 reagent)

2.2.2. Culture, passaging, and cryopreservation of human umbilical vein endothelial cells

2.2.2.1. Cell thawing

Remove the vials containing HUVECs from liquid nitrogen storage, rapidly thaw them in a 37℃ water bath for 1 minute, wipe them with 70% ethanol, and transfer them to a cell culture laminar flow hood. Centrifuge at 800 r/min for 5 minutes, discard the supernatant, add complete culture medium containing 10% fetal bovine serum, and seed the cells into T25 cell culture flasks. Place the culture flask in a cell culture incubator at 37℃ with 5% CO_2. Observe cell morphology after 16 hours; once most cells have adhered to the surface, replace the culture medium and continue culturing for 2–3 days. Under a microscope, the cells are observed to grow as a monolayer, exhibiting a cobblestone-like mosaic arrangement or a short spindle-shaped morphology.

2.2.2.2. Cell passaging

Observe the growth of HUVECs under a microscope. When cell confluence reaches approximately 80%–90%, proceed with cell passaging. Remove the culture medium, rinse twice with sterile PBS, and add an appropriate amount of 0.25% trypsin solution just to cover the cells. If the cells are observed under the microscope to have contracted into round shapes but have not completely detached, immediately add complete medium containing fetal bovine serum to terminate digestion, then pipette the cells off. Centrifuge at 800 r/min for 5 minutes, discard the supernatant, add fresh complete medium, mix thoroughly by pipetting, and passage the cells at a 1:2 ratio.

2.2.2.3. Cell cryopreservation

After passing the cells through 4–5 generations, cryopreserve them in batches. Digest the cells with 0.25%

trypsin solution, add cell cryopreservation medium, and transfer them in batches to sterile cryovials. Perform stepwise freezing at 4℃ for 2 hours, followed by 20℃ for 2 hours, then store at –80℃ overnight. Finally, transfer to a liquid nitrogen tank for long-term storage and label the vials accordingly.

2.2.3. Establishment of a pyroptosis model

Human umbilical vein endothelial cells (HUVECs) were stimulated with 10 μg/mL LPS for 16 h to establish a cellular inflammation model.

When HUVECs undergo inflammatory damage, the intracellular NO signaling pathway is disrupted, leading to changes in NO levels. An NO assay kit was used to measure NO levels in the cell culture supernatants of the control and model groups, respectively.

Collect the supernatant from the HUVEC cell culture media of each group and transfer it to sterile Eppendorf tubes. Centrifuge at 4℃ and 3000 r/min for 15 minutes to remove cell debris and impurities. Pipette the supernatant onto ice for analysis; no additional dilution is required. If a precipitate is present, centrifuge again and collect the supernatant. Dilute the 10 mmol/L standard solution from the NO assay kit with ultrapure water to prepare a gradient of working solutions at 0, 6.25, 12.5, 25, 50, 100, and 200 μmol/L for plotting the standard curve. Arrange blank wells, standard wells, and sample wells sequentially in a 96-well plate, and add 50 μL of the corresponding standard solution or cell culture supernatant to each well. Add 50 μL of Nitrate Reductase Reagent A and 50 μL of Reagent B to each well, mix gently, and incubate at 37℃ for 30 minutes. Add 50 μL of Color Development Solution I to each well and let stand at room temperature for 5 minutes; then add 50 μL of Color Development Solution II, mix thoroughly, and let stand in the dark at room temperature for 15 minutes. Set the microplate reader to a wavelength of 550 nm and measure the absorbance (A value) of each well.

2.2.4. Cell grouping and treatment

Control, model, and low-, medium-, and high-dose muscone groups were established. HUVECs in the 2nd–4th generation logarithmic growth phase were seeded into 6-well cell culture plates at a density of 1×10^6 cells per well, as determined using a cell counter. The plates were incubated in a cell culture incubator (37℃, 5% CO_2). When the cells reached 70%–80% confluence, as observed under a microscope, each well was washed twice with PBS and then treated as follows:

(1) Control group: Cultured in HUVEC-specific medium;
(2) Model group: Cultured in HUVEC-specific medium + 10 μg/mL LPS stimulation for 16 h + HUVEC-specific medium for 24 h
(3) Low-concentration musk ketone group: cultured in HUVEC-specific medium + 10 μg/mL LPS stimulation for 16 h + 1 μmol/L musk ketone for 24 h;
(4) Moderate-concentration musk ketone group: HUVEC-specific medium + 10 μg/mL LPS stimulation for 16 h + 10 μmol/L musk ketone for 24 h;
(5) High-concentration musk ketone group: treated with HUVEC-specific medium + 10 μg/mL LPS stimulation for 16 h + 75 μmol/L musk ketone for 24 h.

2.2.5. ELISA assay for IL-1β and IL-18 levels

Remove the assay kit from refrigeration and allow it to equilibrate to room temperature; prepare the wash buffer in advance according to the mixing ratios specified in the kit instructions, and simultaneously

prepare standard solutions at a concentration gradient and the substrate working solution. Add the standard solutions and test sample solutions sequentially to the pre-set wells of the microplate; seal the plate with a cover film and incubate at room temperature for 2 hours; after incubation, begin washing the plate, repeating the washing process 5 times. Prepare the antibody working solution strictly according to the ratios specified in the manual, add it to all reaction wells, seal the plate with a sealing film, and incubate at 37℃ for 1 hour; after incubation, wash the plate 5 times again. Next, prepare the enzyme-conjugate working solution, dispense according to protocol, seal the plate, and incubate at 37℃ in the dark for 15 minutes. After incubation, first add the color development reagent to each well, then add an equal volume of stopping solution and mix thoroughly to terminate the color development reaction; place the microplate in a microplate reader, select a detection wavelength of 450 nm to measure the OD values of each well, plot a standard curve based on the measured data, use the standard curve to calculate the concentration of the samples under test, and finally perform statistical analysis of the data.

2.2.6. Western blot analysis of the relative expression levels of pyroptosis-related proteins

2.2.6.1. Total protein extraction from venous endothelial cells

Prepare the required volume of lysis buffer in advance, mix thoroughly, and pre-cool on ice. Meanwhile, add 1 mL of lysis buffer to each well containing human umbilical vein endothelial cells, then scrape the cells into Eppendorf tubes using a cell scraper. Use an ultrasonic cell disruptor in an ice bath to sonicate the cells for 3 seconds at a time, with 5-second intervals, for a total of 3 minutes. Set the high-speed centrifuge to 4℃ and 12,000 rpm and pre-cool it in advance; place the lysed human umbilical vein endothelial cells in the centrifuge and centrifuge for 30 minutes. Take a new tube and collect the supernatant after centrifugation. Protein concentration determination: Determine protein concentration using the BCA method. Measure the OD value of the samples at a wavelength of 562 nm, plot a standard curve, and calculate the sample concentration. Measure the volume of the supernatant and add different volumes of RIPA buffer based on the protein concentration to ensure consistent protein concentrations across all groups after dilution. Then, add the protein loading buffer, mix thoroughly, and denature in a 100℃ water bath for 15 minutes.

2.2.6.2. Protein western blotting

Gel Preparation: First, thoroughly clean and air-dry the glass plates and their corresponding frames, then assemble and secure them. Following the operating instructions provided with the gel kit, prepare a 5% loading gel (upper gel) and a 10% separating gel (lower gel) separately. Electrophoresis Procedure: Secure the fully set gel plate in the electrophoresis apparatus. After adding the electrophoresis buffer, slowly remove the comb to prevent damage to the gel in the loading wells. Set a constant voltage of 70 V for a 15-minute pre-electrophoresis. Add the protein samples to be tested in sequence according to the experimental groups, top up the electrophoresis buffer in the outer chamber, and then start the electrophoresis. Membrane Transfer and Blocking: Prepare an adequate amount of transfer buffer in advance and dispense it into the tray and transfer tank, respectively; use a 5 cm × 8 cm PVDF membrane with a pore size of 0.45 μm, and activate it by soaking in methanol for 30 seconds. Remove the gel after electrophoresis is complete, trim and cut it as needed, and soak it in the transfer buffer. Assemble the transfer sandwich according to the stacking order and spray with anhydrous ethanol to thoroughly remove any air bubbles from the sandwich. Cool the perimeter of the transfer system with ice and perform the transfer using a constant current of 300 mA; adjust the

transfer duration based on the molecular weight of the target protein. After the transfer is complete, incubate the gel with a 5% skim milk blocking solution at room temperature for 1 hour. Antibody Incubation: Wash three times with 1× TBST (8 min per wash). Dilute the NLRP3 (1:2000), GSDMD (1:2000), and Caspase-1 (1:70,000) antibodies according to the specified ratios, then incubate the membrane in the diluted antibody solution at 4℃ overnight. The next day, remove the primary antibody, wash the membrane three times with 1×TBST (8 min per wash), and incubate it in the secondary antibody (1:3,000) at room temperature for 1 hour. Finally, wash the membrane three times with 1×TBST (8 min per wash). Color Development: Prepare the developing solution by mixing components A and B in a 1:1 ratio according to the kit instructions. Place the PVDF membrane in a color development plate, add the developing solution dropwise to develop the signal, and capture the image.

3. Results

3.1. Experimental results

3.1.1. Calculation of cell survival rate using the CCK-8 cell viability assay

As shown in **Figure 1**, the results indicate that cell viability was consistently greater than 75%. Musk ketone exhibited no IC_{50} across the concentration range of 1 μmol, 5 μmol, 10 μmol, 25 μmol, 50 μmol, and 75 μmol; within this concentration range, musk ketone did not produce a significant inhibitory effect on cell proliferation.

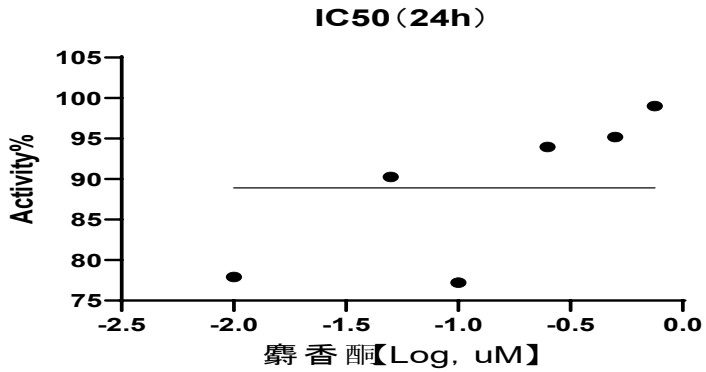


Figure 1. Cell viability after treatment with different concentrations of musk ketone.

3.1.2. Determination of NO levels in cell culture supernatant

As shown in **Figure 2**, compared with the control group, the NO content in the cell supernatant of the LPS model group increased significantly after 16 hours of treatment with 10 μg/mL LPS ($P < 0.001$).

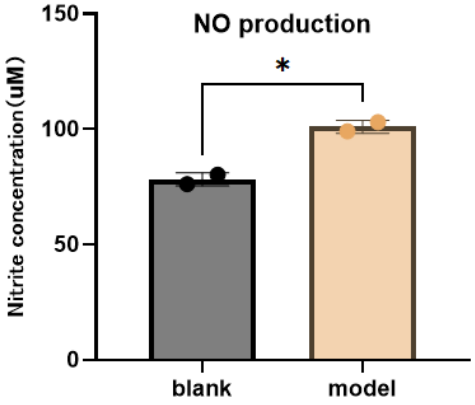


Figure 2. Comparison of NO levels in cell culture supernatant. Note: Comparison between the control group and the LPS model group, ***$P < 0.001$.

3.1.3. Detection of IL-18 and IL-1β expression in cells by enzyme-linked immunosorbent assay (ELISA)

Enzyme-linked immunosorbent assay (ELISA) was used to detect the expression levels of IL-18 and IL-1β in cells. As shown in **Table 3**, the expression levels of IL-18 and IL-1β in the model group were significantly higher than those in the control group, with a statistically significant difference ($P < 0.05$). Compared with the model group, the low-, medium-, and high-dose musk ketone groups all showed reduced IL-18 expression, with statistically significant differences ($P < 0.05$); compared with the model group, the high- and low-dose musk ketone groups both showed reduced IL-1β expression, with statistically significant differences ($P < 0.05$); compared with the model group, the medium-dose group of musk ketone showed a reduction in IL-1β expression, but the difference was not statistically significant ($P > 0.05$). In summary, the results indicate that the expression levels of the inflammatory factors IL-18 and IL-1β in cells increased after LPS stimulation, and musk ketone can reduce the levels of these inflammatory factors in cells.

Table 3. Detection of IL-18 and IL-1β expression in cells by ELISA (mean ± SD)

Group	IL-18 (pg/mL)	IL-1β (pg/mL)
Blank Group	41.89 ± 2.077	33.50 ± 2.121
Model group	82.69 ± 3.266###	45.30 ± 4.313#
High-dose musk ketone group	60.77 ± 1.185*	34.45 ± 1.492*
Musk ketone medium-dose group	59.14 ± 7.749**	36.31 ± 0.9758
Low-dose group of musketone	65.11 ± 1.258*	35.03 ± 1.449*

Note: * $P < 0.05$ compared with the model group; ** $P < 0.01$ compared with the model group; # $P < 0.05$ compared with the blank group; ### $P < 0.001$ compared with the blank group

The expression levels of IL-18 and IL-1β in cells were detected using an enzyme-linked immunosorbent assay (ELISA). The results in **Figure 3** show that, compared with the blank group, the model group exhibited a statistically significant increase in IL-18 expression ($P < 0.001$); the low-, medium-, and high-dose musk ketone groups all exhibited a statistically significant reduction in IL-18 expression compared with the model group ($P < 0.05$).

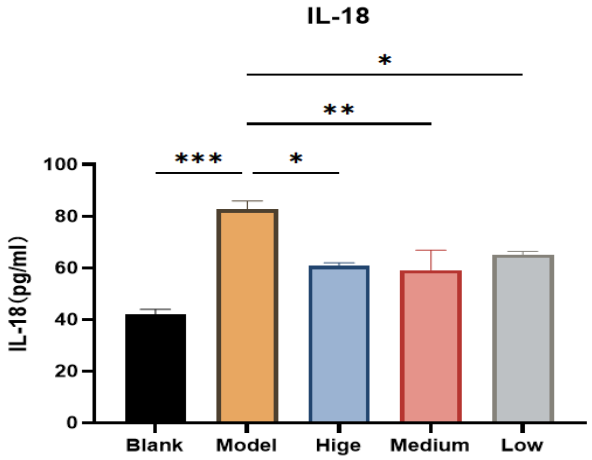


Figure 3. Expression levels of IL-18 in cells. Note: Compared with the model group: ***$P < 0.001$; **$P < 0.01$; *$P < 0.05$; ns $P > 0.05$.

Figure 4 shows that, compared with the control group, the model group exhibited a statistically significant increase in IL-1β expression ($P < 0.05$); Compared with the model group, IL-1β expression was reduced in both the high-dose and low-dose musk ketone groups, with statistically significant differences ($P < 0.05$); there was no significant difference in IL-1β expression between the model group and the medium-dose musk ketone group ($P > 0.05$).

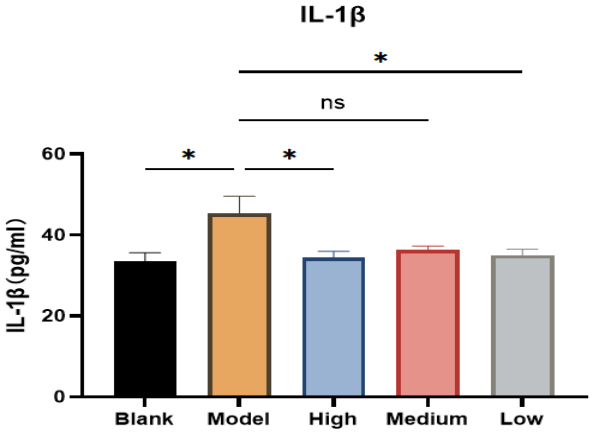


Figure 4. IL-1β expression levels in cells. Note: Compared with the model group: ***$P < 0.001$; **$P < 0.01$; *$P < 0.05$; ns $P > 0.05$.

3.1.4. Western blot analysis of relative expression levels of pyroptosis-related proteins in cells from each group

Table 4. Comparison of relative expression levels of pyroptosis-related proteins in cells across groups (mean ± SD)

	NLRP3	Caspase-1	Gasdermi D
Blank	1.427 ± 0.1797	0.5007 ± 0.0918	0.6128 ± 0.0221

Model	2.229 ± 0.1227##	0.7367 ± 0.0404#	0.8048 ± 0.0414##
High	1.724 ± 0.643*	0.5175 ± 0.0509*	0.6300 ± 0.0424*
Medium	1.689 ± 0.2524*	0.4660 ± 0.0814**	0.6475 ± 0.0671*
Low	1.675 ± 0.0756*	0.4427 ± 0.0593**	0.6118 ± 0.0209**

Note: Statistical data represent the mean ± standard deviation from at least three independent experiments. (Compared with the control group, # indicates $P < 0.05$, and ## indicates $P < 0.01$; compared with the model group, * indicates $P < 0.05$, ** indicates $P < 0.01$, *** indicates $P < 0.001$, and ns indicates $P > 0.05$)

Figure 5 shows that, compared with the control group, the model group exhibited a statistically significant increase in intracellular NLRP3 protein expression ($P < 0.01$); compared with the model group, the high-, medium-, and low-dose muscone groups all exhibited a statistically significant reduction in intracellular NLRP3 protein expression ($P < 0.05$). In summary, the results indicate that LPS stimulation increases NLRP3 protein expression in cells, and musk ketone can reduce NLRP3 protein expression in cells.

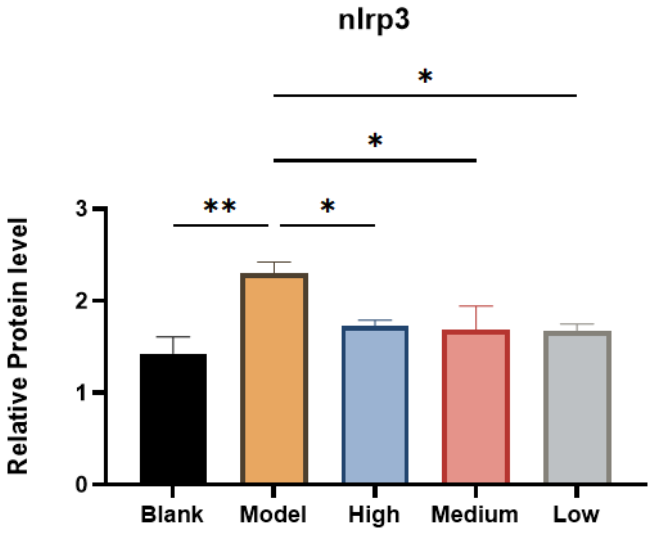


Figure 5. Relative levels of NLRP3 protein expression. Note: Compared with the model group: ***$P < 0.001$; **$P < 0.01$; *$P < 0.05$; ns $P > 0.05$.

Figure 6 shows that, compared with the model group, Caspase-1 protein expression in cells increased in the blank group, and the difference was statistically significant ($P < 0.05$); compared with the model group, Caspase-1 protein expression decreased in the high-, medium-, and low-dose muscone groups, and the differences were statistically significant ($P < 0.05$).In summary, the results show that LPS stimulation increases Caspase-1 protein expression in cells, and musk ketone can reduce Caspase-1 protein expression in cells.

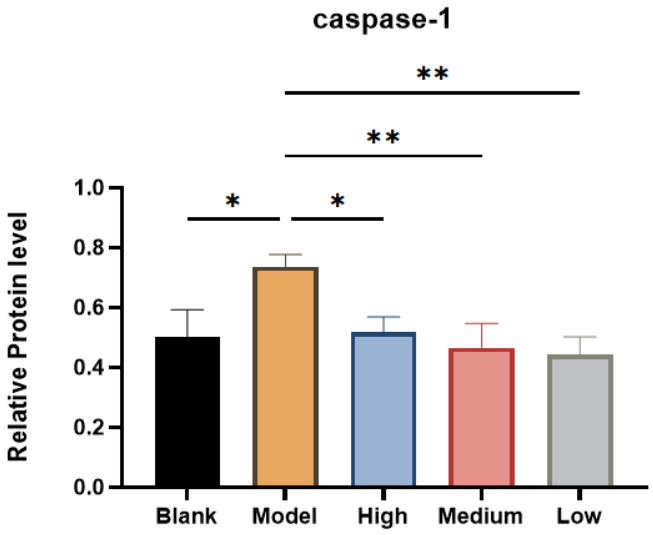


Figure 6. Relative levels of Caspase-1 protein expression.Note: Compared with the control group, ***$P < 0.001$; **$P < 0.01$; *$P < 0.05$; ns $P > 0.05$.

The results in **Figure 7** show that GSDMD protein expression in the model group was significantly higher than that in the control group ($P < 0.01$); in contrast, GSDMD protein expression in the high-, medium-, and low-concentration muskon groups was significantly lower than that in the model group ($P < 0.05$). In summary, the results indicate that LPS stimulation increases GSDMD protein expression in cells, and musk ketone can reduce GSDMD protein expression in cells.

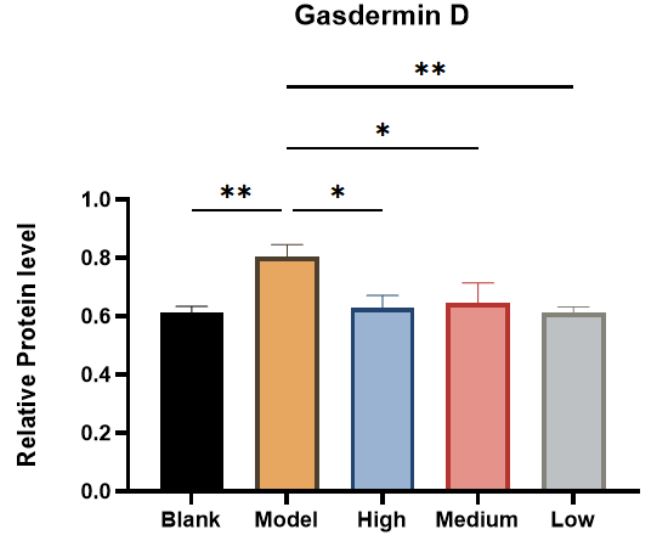


Figure 7. Relative GSDMD protein expression.Note: Compared with the model group, **$P < 0.001$; **$P < 0.01$; *$P < 0.05$; ns $P > 0.05$.

4. Conclusions and Outlook

4.1. Conclusions

4.1.1. Screening for safe concentrations of muscone using the CCK-8 assay

After 24 hours of treatment with different concentrations of muscone in HUVECs, the cell survival rate remained > 75% in all cases, with no significant cytotoxicity observed and no IC_{50} detected. This indicates that the concentration range used in the experiment is safe and reliable and can be applied in subsequent mechanistic studies.

4.1.2. Validation of the LPS-induced pyroptosis model in HUVECs

Compared with the control group, NO levels in the cell culture supernatant of the LPS model group were significantly elevated, confirming that LPS successfully induced pyroptosis and inflammatory damage in endothelial cells.

4.1.3. Enzyme-linked immunosorbent assay (ELISA) was used to detect the levels of IL-18 and IL-1β in the cells

The levels of IL-18 and IL-1β in the model group were higher than those in the control group, confirming the successful establishment of the pyroptosis model; the model group exhibited reduced IL-18 expression compared to the low-, medium-, and high-concentration muskone groups; the low-, medium-, and high-dose muskone groups showed reduced IL-1β expression compared to the model group, although this reduction was not significant in the medium-dose muskone group. In summary, the results indicate that musk ketone can reduce the levels of the inflammatory cytokines IL-18 and IL-1β in cells and, to a certain extent, alleviate the severity of LPS-induced pyroptosis in human umbilical vein endothelial cells.

4.1.4. Western blot analysis of the relative expression levels of pyroptosis-related proteins in each group

Compared with the blank control group, the model group exhibited increased expression levels of GSDMD, NLRP3, and Caspase-1 proteins, confirming the successful establishment of the pyroptosis model; in contrast, the high-, medium-, and low-dose musk ketone groups showed reduced expression levels of Caspase-1, NLRP3, and GSDMD proteins compared with the model group.

In summary, the results show that in the model group treated with LPS, the protein expression levels of NLRP3, GSDMD, and Caspase-1 were all elevated, indicating that LPS induced pyroptosis and that the pyroptosis model was successfully established and exacerbated the inflammatory response. In contrast, the high-, medium-, and low-dose groups of musk ketone significantly reduced the expression of pyroptosis-related proteins NLRP3, GSDMD, and Caspase-1, exerting a certain inhibitory effect on LPS-induced pyroptosis. This suggests that musk ketone inhibits pyroptosis by regulating the NLRP3, GSDMD, and Caspase-1 signaling pathways.

4.2. Discussion

Diabetic ulcers, as a common, intractable, and severe complication of diabetes, are characterized primarily by delayed resolution of wound inflammation, vascular endothelial damage, and impaired repair processes; an overactivated inflammatory response is the core factor contributing to prolonged non-healing of the wound. Pyroptosis is a form of programmed inflammatory cell death dependent on the NLRP3/Caspase-1/

GSDMD signaling pathway. It involves membrane perforation and cell lysis, leading to the release of large amounts of pro-inflammatory factors such as IL-1β and IL-18, which trigger an inflammatory cascade. This further damages the structure and function of the vascular endothelium and exacerbates disruptions in the wound microenvironment. Pyroptosis has thus become a key target in recent research on the mechanisms of diabetic complications. Endothelial cells are key cells that maintain vascular homeostasis and participate in wound angiogenesis and tissue repair. Human umbilical vein endothelial cells (HUVECs), with their stable biological characteristics and good reproducibility in in vitro culture, serve as an ideal cellular model for studying endothelial inflammatory damage and pyroptosis. In this study, LPS was used to induce HUVECs to establish an in vitro inflammatory pyroptosis model. We investigated the regulatory role of muscone in endothelial cell pyroptosis and its potential molecular mechanisms, providing experimental support for the application of muscone in the prevention and treatment of hard-to-heal diabetic wounds.

Musk ketone is the core active compound in natural musk and possesses multiple pharmacological activities, including anti-inflammatory, antioxidant, and vascular endothelial protective effects. Existing studies have confirmed that it can alleviate inflammatory damage in multiple organs, such as the myocardium and kidneys, by inhibiting the activation of the NLRP3 inflammasome. In this study, the CCK-8 assay was used to screen for the cytotoxic effects of muscone at concentrations ranging from 1 to 75 μmol/L on HUVECs. The results showed that cell survival rates in all concentration groups exceeded 75%, with no significant inhibition of proliferation or cytotoxicity, confirming good safety within this concentration range and establishing a concentration basis for subsequent pharmacological intervention experiments.

LPS is a classic inducer of in vitro cellular inflammation and pyroptosis models. Following the literature, this study used 10 μg/mL LPS to stimulate HUVECs for 16 hours to establish a pyroptosis model. After LPS stimulation, cellular NO and inflammatory cytokine levels increased significantly, consistent with the characteristics of an endothelial cell pyroptosis-inflammation model and in line with modeling conditions and phenotypes reported in previous literature. Enzyme-linked immunosorbent assay (ELISA) results showed that IL-1β and IL-18 secretion levels in the LPS model group were significantly higher than those in the control group, indicating that LPS promotes the massive release of pro-inflammatory factors by activating the pyroptosis pathway, thereby mediating endothelial inflammatory damage; musk ketone significantly downregulated the expression of IL-1β and IL-18. Western blot results further elucidated the mechanism of action of musk ketone at the protein molecular level. LPS treatment significantly upregulated the expression of key proteins in the pyroptosis pathway—NLRP3, Caspase-1, and GSDMD—indicating that LPS activates the classical NLRP3/Caspase-1/GSDMD pyroptosis pathway, thereby inducing pyroptosis in HUVECs.Musk ketone treatment significantly downregulated the expression of Caspase-1, GSDMD, and NLRP3 proteins. It is hypothesized that musk ketone primarily acts by inhibiting the initiation of NLRP3 inflammasome activation, thereby suppressing Caspase-1 activation, reducing GSDMD proteolytic cleavage, and decreasing cell membrane pore formation and pyroptosis, which in turn inhibits the release of pro-inflammatory factors such as IL-18 and IL-1β.

4.3. Limitations and Future Directions

This study was conducted solely in an in vitro single-cell model using HUVECs and thus has several limitations: First, the regulatory effects of different concentrations of muscone on LPS-induced pyroptosis and inflammatory cytokine expression in HUVECs did not exhibit a uniform gradient pattern, likely due

to the lack of validation with a more refined concentration gradient. Second, the study did not simulate the actual pathological microenvironment of high glucose combined with LPS in diabetic patients; the absence of a combined high-glucose plus LPS induction model results in a certain discrepancy from the actual pathological state of diabetic ulcers. Third, the study assessed key pyroptosis pathway markers only at the protein expression level and did not examine the mRNA transcription levels of NLRP3, Caspase-1, GSDMD, IL-1β, IL-18, and other molecules at the genetic level, resulting in an incomplete analysis of the molecular mechanisms. Fourth, the study focused solely on pyroptosis and inflammatory responses, without investigating the effects of muscone on HUVEC proliferation, migration, and tubule formation, as well as wound-healing-related biological behaviors such as oxidative stress, apoptosis, and autophagy. Fourth, there is a lack of in vivo animal experiments; no animal model of diabetic ulcers was established, making it impossible to verify the in vivo pharmacological effects and pathway regulatory roles of muscone at the levels of histopathology and wound healing rates.

Based on the results of this study and the limitations of existing research, future studies could be expanded in multiple dimensions: First, future research could narrow the concentration range and establish a denser concentration gradient to further precisely define the effective concentration range of muscone for protecting endothelial cells and inhibiting pyroptosis, thereby refining its dose-dependent mechanism of action and making the experimental conclusions more rigorous and comprehensive. Second, a model of HUVEC damage induced by a combination of high glucose and LPS could be established to more closely mimic the in vivo pathological microenvironment of diabetic ulcers, thereby further clarifying the regulatory role of musk ketone in endothelial pyroptosis induced by high glucose combined with inflammation. Third, integrate techniques such as PCR, immunofluorescence, and immunoprecipitation to elucidate the specific molecular mechanisms by which musk ketone regulates the NLRP3/Caspase-1/GSDMD pathway at the levels of genes, proteins, cellular localization, and protein interactions; combine this with intervention using pathway inhibitors to pinpoint the key targets of its action. Fourth, we will broaden the scope of research parameters to investigate the effects of muscone on HUVEC proliferation, migration, angiogenesis, oxidative stress, apoptosis, and macrophage polarization, thereby comprehensively elucidating its multi-target role in promoting diabetic wound healing; Fifth, establish in vivo rat and mouse models of diabetic ulcers and, through wound healing observations, hematoxylin-eosin (HE) staining of tissues, and immunohistochemistry, validate the pharmacological effects of muscone in inhibiting endothelial pyroptosis, alleviating inflammatory damage, and promoting wound healing in animals.

Funding

This work has been supported by Medical and Health Science and Technology Project of Shandong province (Project No.: 202302040939).

Disclosure statement

The author declares no conflict of interest.

References

[1] Li ZH, Xu C, Gui H, 2024, Advances in Clinical Treatment Research on Diabetic Foot. Electronic Journal of Foot and Ankle Surgery, 11(02): 68–73.

[2] Shi FT, Shen JQ, Wu MJ, 2024, Advances in Research on the Pathogenesis of Diabetic Non-healing Wounds. Life Sciences, 36(04): 509–516.

[3] Zhu SL, Ge XY, Yang YL, et al., 2024, Research Progress on Pyroptosis in Diabetic Wound Healing. Journal of Hainan Medical University, 30(06): 469–474.

[4] Chen ZC, Lin QN, Yang YF, et al., 2024, The Role of Pyroptosis in Diabetes and Its Complications and Advances in Traditional Chinese Medicine Interventions. Chinese Herbal Medicines, 55(20): 7180–7191.

[5] Zeng YY, Jiang H, Tang WY, 2026, Effects of Matrine on Inflammatory Damage to Endothelial Cells in Rats with Coronary Heart Disease via Regulation of the cGAS/STING/NF-κB Signaling Pathway. Hebei Medicine, 48(6): 890–894.

[6] Cao J, 2023, Mechanistic Study on CIRCpedia_4214's Regulation of Microglia Pyroptosis Following Spinal Cord Injury via the miR-212-5p/Myd88 Axis, thesis, Nanchang University.

[7] Li P, Huang JK, Li CS, et al., 2026, Effects of Yixiao Formula on the NLRP3/Caspase-1/GSDMD Pyroptosis Pathway in Mice with Diabetes and Fatty Liver. Global Traditional Chinese Medicine, 19(3): 505–511.

[8] Wang T, Fan LH, Chen B, et al., 2022, Study on the Role of the NLRP3-NF-κB Inflammatory Signaling Pathway in Pyroptosis of Cells in Diabetic Foot Wounds. Advances in Modern General Surgery in China, 25(10): 795–799.

[9] Jiang FY, 2024, A Study on the Effects and Mechanisms of Yuzhu Polysaccharides in Improving Diabetic Nephropathy by Regulating the SIRT1/NLRP3/Caspase-1 Signaling Pathway, thesis, Changchun University of Traditional Chinese Medicine.

[10] Zhou J, 2023, Inhibition of Pyroptosis in Islet β-Cells of Diabetic Mice by Rhodiola Glucoside via Regulation of the NLRP3/GSDMD Signaling Pathway, thesis, Hubei Medical University.

[11] Zhao L, Liu YZ, Wang Y, et al., 2024, Establishment of a Model of Lipopolysaccharide-Induced Inflammatory Injury in Small Intestinal Epithelial Cells of Piglets. Journal of Heilongjiang Bayi Agricultural University, 36(03): 50–57.

[12] Wang ZY, Tian DY, Zheng P, et al., 2025, Muscone Improves Coronary Microvascular Disease by Promoting Microvascular Formation Mediated by VEGF Expression. Journal of the Army Medical University, 47(19): 2374–2384.

[13] Yang XL, Chang Y, Guo DX, et al., 2025, Advances in Research on the Pharmacological Effects of Muscone. Chinese Pharmaceutical Industry, 34(5): 129–133.

[14] Wu X, 2023, Design, Construction, and Application Research of a Muskone-Regulated Genetic Circuit, thesis, East China Normal University.

[15] Yao G, 2025, Recent Advances in Research on the Antioxidant Effects of Muscone. Shandong Chemical Industry, 54(3): 110–112, 115.

[16] Shi YQ, Lei YH, 2023, Study on the Mechanism of Action of Muscone on Myocardial Injury in Mice with Sepsis. Journal of Cardiovascular and Cerebrovascular Diseases in Integrated Traditional and Western Medicine, 21(19): 3540–3544.

[17] Zhang K, Zhao CL, Pan L, et al., 2026, Mechanism of Action of Qi Ju Di Huang Wan in the Treatment of Diabetic

Retinopathy via the NLRP3/Caspase-1/GSDMD Signaling Pathway. Chinese Journal of Experimental Formulary, 1–11.

[18] Ai JW, Xu DH, Chen YF, et al., 2024, Research Progress on Lipopolysaccharide in the Construction of Poultry Stress Models. Today's Animal Husbandry and Veterinary Medicine, 40(10): 74–76.

[19] Ran ZQ, Liu ZH, Yang R, et al., 2026, Research Progress on the Role and Mechanisms of Pyroptosis in Diabetic Nephropathy. Journal of Kunming Medical University, 47(1): 148–156.

[20] Tian XR, Tang QL, 2022, Recent Advances in the Mechanisms of Lipopolysaccharide and Fibroblasts in Wound Healing. Chinese Journal of Burns and Wounds, 34(04): 236–239.

[21] She X, Li XJ, Huang HX, et al., 2026, Lipopolysaccharide Regulates the Function of Human Umbilical Vein Endothelial Cells. Chinese Journal of Tissue Engineering, 30(13): 3280–3287.

[22] Liu PF, 2016, A Study on the Role of Muscone in Augmenting the Therapeutic Effect of Bone Marrow Mesenchymal Stem Cells on Acute Kidney Injury in Rats, thesis, Jilin University.

Publisher's note

Bio-Byword Scientific Publishing remains neutral with regard to jurisdictional claims in published maps and institutional affiliations.